

# THERMOGRAPHIC MONITORING OF ALUMINIUM FOAMING PROCESS

E. Solórzano<sup>1 † \*</sup>, F. Garcia-Moreno<sup>1,2</sup>, N. Babcsán<sup>3</sup>, J. Banhart<sup>1,2</sup>

<sup>1</sup> *Institute of Applied Materials, Helmholtz-Zentrum Berlin, Glienicker Straße 100, 14109 Berlin, Germany*

<sup>2</sup> *Technical University Berlin, Hardenberg Strasse 36, 10623 Berlin, Germany*

<sup>3</sup> *BayLOGI, Bay Zoltan Foundation for Applied Research, Miskolc-Tapolca 3519, Iglói u. 2., Hungary*

\*Corresponding author, e-mail: esolo@fmc.uva.es

† *Former institution: CellMat Laboratory, University of Valladolid, Prado de la Magdalena S/N 47011*

*Valladolid, Spain*

## ABSTRACT

A novel method for measuring the temperature distribution and evolution of metal foams in the molten state is proposed. Foamable AlSi9 precursor material containing 0.6 wt.% TiH<sub>2</sub> was foamed, kept at high temperatures and solidified while its temperature distribution was monitored by a thermographic camera. Free foaming and foaming inside a closed mould were carried out and direct and screened IR monitoring have been tested. Different heating conditions were applied giving rise to homogeneous and inhomogeneous temperature distributions. The effect of oxidation was studied on a piece of pure aluminium for reference purposes. The error sources of the measured temperature were analysed. Direct monitoring of foams was shown to be associated to serious problems with quantitative temperature measurement, while screened monitoring yielded promising and accurate quantitative results.

**Keywords:** thermography, aluminium, foam

# 1 INTRODUCTION

Metal foams are potential materials for a number of engineering applications, promoted not only by single mechanical or physical properties but by the combination of such properties <sup>[1]</sup>. Unfortunately, many foaming routes have not yet reached sufficient maturity and foams produced still suffer substantial deficiencies <sup>[2]</sup>. For this reason, some possible applications have not been put into reality. Foamed metals have been intensely studied in the past 10 years, which has led to knowledge about the fundamentals of foaming and foam stability <sup>[3,4,5,6]</sup> and to the development of alternative foaming strategies <sup>[7,8,9]</sup>. Still, there is some need to study the foaming process in more detail to be able to improve manufacture of such materials.

Especially in the production of large foam parts via the powder metallurgical (PM) route the foaming process suffers from the critical effect of temperature distributions which give rise to structural defects and local foam collapse <sup>[10]</sup>. Uniform temperature distributions are more difficult to obtain the larger the piece to be foamed is. Therefore, a method to measure and control temperature inhomogeneties can help in upscaling aluminium foam production.

Temperature can affect the foaming kinetics, foam stability in the liquid state and foam solidification in different ways. Blowing agent decomposition <sup>[11,12]</sup>, the molten metal viscosity and surface tension <sup>[13]</sup> and bubble pressure gradients are influenced by temperature.

Different approaches can be considered to study the temperature distribution during the foaming process of aluminium. Using an array of thermocouples to register the

temperature in different areas during the foaming seems to be the simplest method <sup>[14]</sup>. Nevertheless, a physical contact between the foaming melt and the thermocouples is required, which is difficult to ensure as the foam is moving while the thermocouples have to be kept in fixed positions. Non optimum thermal contacts or an influence on foaming as the thermocouples might act as mechanical barrier or heat sinks and the influence of the container in which the foam is kept can complicate the seemingly simple measurement.

The second approach is using contactless methods for temperature measurement. IR temperature detectors are admitted to be adequate to measure high temperatures with acceptable accuracy <sup>[15]</sup>. An additional advantage can be obtained if a matrix of detectors is used to acquire the temperature with spatial resolution. This method is called “infrared thermography” since the temperature data is generated as a 2D image in which the pixel value represents temperature.

Thermographic techniques have been successfully applied to monitor other processes in which the temperature is a key factor as in polymer and metal welding processes as well as in permanent mould casting <sup>[16,17,18]</sup>. Moreover, the heat transport properties of solid foams have been studied with this technique <sup>[19]</sup>. Nevertheless, this is the first time thermography has been applied to monitor *in-situ* the temperature distribution during the foaming of metals quantitatively.

## 2 EXPERIMENTAL

### 2.1 Fundamentals of far infrared thermography

Infrared cameras are based on 2D arrays of microbolometers (or semiconductor sensors for the near-mid infrared) which detect individually the temperature of a given region. Each element of the array comprises a microresistor which changes its resistance as it heats up as a result of the IR radiation absorbed. The camera electronics convert the changes in resistance to the final thermal image. A lens needs to be placed in between the monitored object and the detector to obtain a focused thermal image. The transmittance characteristics of the lens restrict the wavelength range in which the camera is sensitive for radiation.

The object to be monitored radiates in a wide range of wavelengths with the maximum of radiance corresponding to its own temperature as predicted by Wien's displacement law. As the emitting object is not a black-body the theoretical emitted spectral energy distribution needs to be multiplied by the surface emissivity of the object ( $\epsilon$ ). The higher the temperature is, the more total energy is emitted at lower average wavelengths, in accordance with both Stefan-Boltzmann's and Wien's laws.

A schematic drawing is given in Fig. 1, showing all the factors that influence the final thermal image. The energy reaching the sensor,  $W_T$ , is not only a contribution of the object since also both the surroundings and the atmosphere emit energy that needs to be taken into account. The energy  $W_{\text{sur}}$  radiated by the surroundings is reflected by the object according to its reflectivity  $R=1-\epsilon$ . As a result, the object not only irradiates according to its temperature and emissivity but also reflects radiation from the

surroundings. Furthermore, the atmosphere in between the object and the infrared camera modifies the two radiative contributions from the object, given by its transmittance  $\tau$ , and also radiates energy itself ( $W_{atm}$ ) thus contributing with a certain amount of energy.

The energy emitted by the object ( $W_{obj}$ ) can therefore be expressed in terms of the total energy reaching the camera and the contributions by both atmosphere and surroundings<sup>[20]</sup>:

$$W_{obj} = \frac{1}{\varepsilon\tau} W_T - \frac{1-\tau}{\tau} W_{sur} - \frac{1-\tau}{\varepsilon\tau} W_{atm} \quad (1)$$

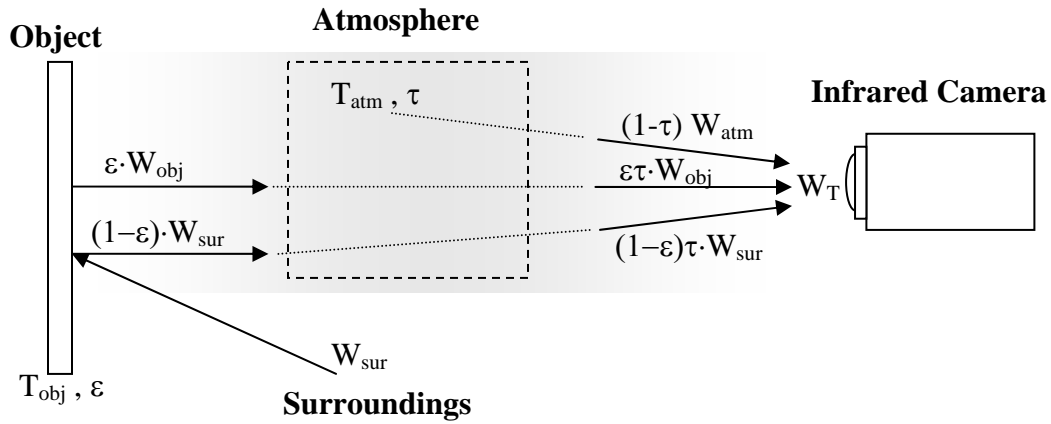


Figure 1

Note that  $W_{sur}$  and  $W_{atm}$  are spurious contributions and usually are tried to be controlled and reduced to improve the signal to noise ratio.

Due to the camera's internal calibration it is possible to transform the energy received in the operating IR range into temperature. The temperature read by the camera only depends on two adjustable parameters *object emissivity* and the *atmosphere transmittance* as shown in eq.1.

If the object emissivity is low it is more difficult to measure accurately the temperature since the other contributions are in the same order of magnitude. Therefore, it is important to maximise surface emissivity. Nevertheless, it is not just a high emissivity which facilitates measuring the temperature of an object, but also a constant emissivity in the entire area under study and a smooth and optimally oriented surface, i.e. perpendicular to the focusing direction. Under any other condition (rough or curved surfaces, non-constant emissivity, etc.) the thermal images obtained will contain temperature inaccuracies. It is also important to mention that with an integral emissivity adjustment as usually found in IR cameras it is not possible to measure accurately the temperature of two objects with a different emissivity in the same thermal image using the same calibration.

The material to be inspected by IR thermography in the present study – aluminium and aluminium foam – will not be ideal in the sense just described since it presents a high variance in its emissivity. Polished aluminium has a very low emissivity ranging from 0.03 to 0.06, whereas oxidised or even anodised aluminium shows an emissivity in an ever wider range (0.1 to 0.4 and 0.1 to 0.85 for oxidised and anodised surfaces, respectively) <sup>[21]</sup>. The foams studied will exhibit a variety of oxidation conditions and therefore a broad range of values for  $\epsilon$ .

## **2.2 Measurement method**

A far infrared camera by FlirSystems, model “Thermovision A40M”, has been used to acquire the surface temperature of the samples during the heating, foaming and solidification stages. The camera has a 320×240 microbolometer matrix and was used at a

working distance of 30 cm. It was operated in a temperature range from 300 °C to 1500 °C and thermographic images were acquired at 12.5 fps. Additional thermocouples have been used to adjust the emissivity of the samples monitored.

For preparing aluminium foams a powder mixture of AlSi9 and 0.6 wt.% of TiH<sub>2</sub> was hot-compacted to a dense precursor, which upon heating was transformed into a foam as described, e.g., in [1]. In addition, a piece of conventional 99.9 % pure aluminium was used to study the influence of progressive oxidation on emissivity while this piece was being kept at high temperature for a long period.

The schematic description of the heating conditions is shown in Fig. 2. Besides direct free foaming on a ceramic heater (a), two additional heating set-ups have been used to heat the samples under homogeneous and inhomogeneous conditions: The mould heated from the bottom by a heating plate provides a non-uniform temperature distribution in the vertical direction (b). Three near/mid-infrared heating lamps were used to heat the sample indirectly through a mould, trying to produce a more homogeneous heating (c). The lamps heat directly only the parts of the mould that are not touching the sample. Therefore, punctual overheating of the precursor is avoided and the heating process is governed by slow thermal conduction processes. The infrared heating lamps do not disturb the temperature reading since they emit in a different spectral range.

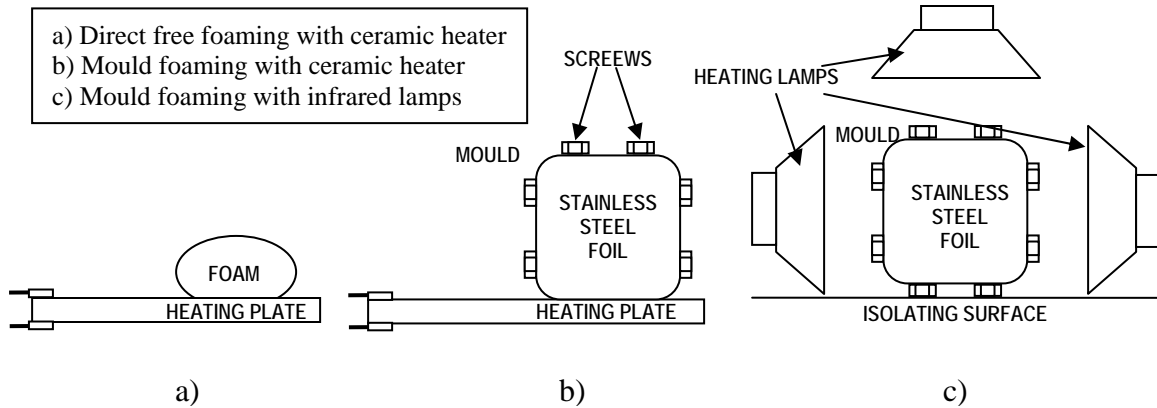


Figure 2

A hollow profile made of stainless steel –  $30 \times 30 \text{ mm}^2$  cross section, 3 mm wall thickness, 28 mm length – containing the foamable samples inside, was used as mould in most of the experiments. Optionally, the two open ends of the mould were covered with a  $25 \mu\text{m}$  thick stainless steel foil which acted as screen preventing a direct view on the foam by the camera. The foil, in contact with the sample inside, was sprayed with graphite outside to optimise emissivity and to improve the accuracy of temperature measurement as it will be shown later.

The final images obtained were analysed by using ImageJ software <sup>[22]</sup>. The spatially averaged temperature change with time and the temperature profiles were obtained by using some special functions programmed by the authors.

### 3 RESULTS and DISCUSSION

The three steps (foaming, holding in molten state and solidification) occurring during foam evolution are analysed in this section. It is important to mention that we have assigned the term *foaming* to describe the growing step of the foam and not the entire process.

#### 3.1 Foaming

Free foaming of a precursor material induced by inhomogeneous heating from the bottom by a ceramic heater on which the foam was placed was monitored by the infrared camera. Previous calibrations recommended fixing the surface emissivity to 0.25. The foaming is shown at different times in Fig. 3. It is important to note that this emissivity is adjusted for the metal surface which means the temperature is not the real one for other objects with other emissivity. The emissivity of the ceramic heating plate is higher and, as a consequence, its temperature cannot be measured simultaneously and an artificial reading of 1500 °C is obtained. In the foam part, newly evolving unoxidised surfaces with a very low and differing emissivity compared to the rest of the surface can be observed as black fan-shaped features.

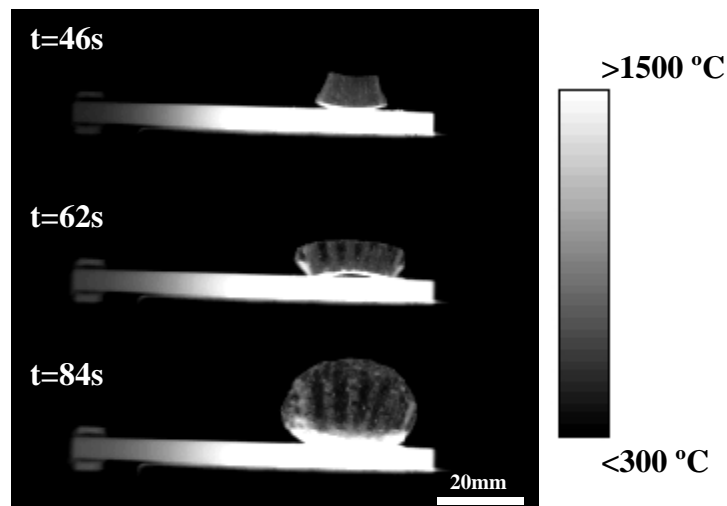


Figure 3

The average apparent temperature and their standard deviation have been measured on the foam surface in three of the thermographs by spatial averaging. The apparent IR temperatures with increasing time were  $619\pm 44$  °C,  $592\pm 117$  °C and  $577\pm 175$  °C for  $t = 46$  s,  $62$  s and  $84$  s, respectively. Therefore, it is clear that the new unoxidised surfaces being increasingly generated during expansion both reduce the apparent temperature and give rise to a pronounced increase of the standard deviation of temperature.

To solve this problem a material with a constant-high emissivity and very *low thermal capacity* was put into *permanent contact* with the growing foam. A graphite-sprayed  $25$   $\mu\text{m}$  thick stainless steel foil was used for this purpose. After the calibrations had been carried out, the emissivity was adjusted to a value of  $0.85$ . As the surface is plane and the emissivity is constant and high, we can expect an accurate temperature measurement. In addition, the contact between the sample and the foil was ensured: the precursor material touched the foil from the beginning and, as it was expanding, the contact was permanent throughout the process. In order to avoid the foil to move due to foam expansion it was tightened to the mould by several screws (see Fig. 2 b and c) that ensured the flatness and the initial contact as well. The foaming behaviour was checked in experiments with and without using the steel foil, yielding very similar results.

Fig. 4 illustrates the foaming pattern under homogeneous (a) and inhomogeneous (b) heating conditions. For homogeneous heating, the sample starts to expand in the hottest top and lateral surfaces. Foaming is completed after about 1 min and a homogeneous temperature distribution is reached. In contrast, if the sample is bottom-heated (Fig. 4.b), it foams first at the bottom part and a permanent temperature gradient from bottom to top

is created. After 1 min maximum expansion seems to have been reached and liquid metal overflows even though in the top part the foam has not touched the thin metallic screening foil.

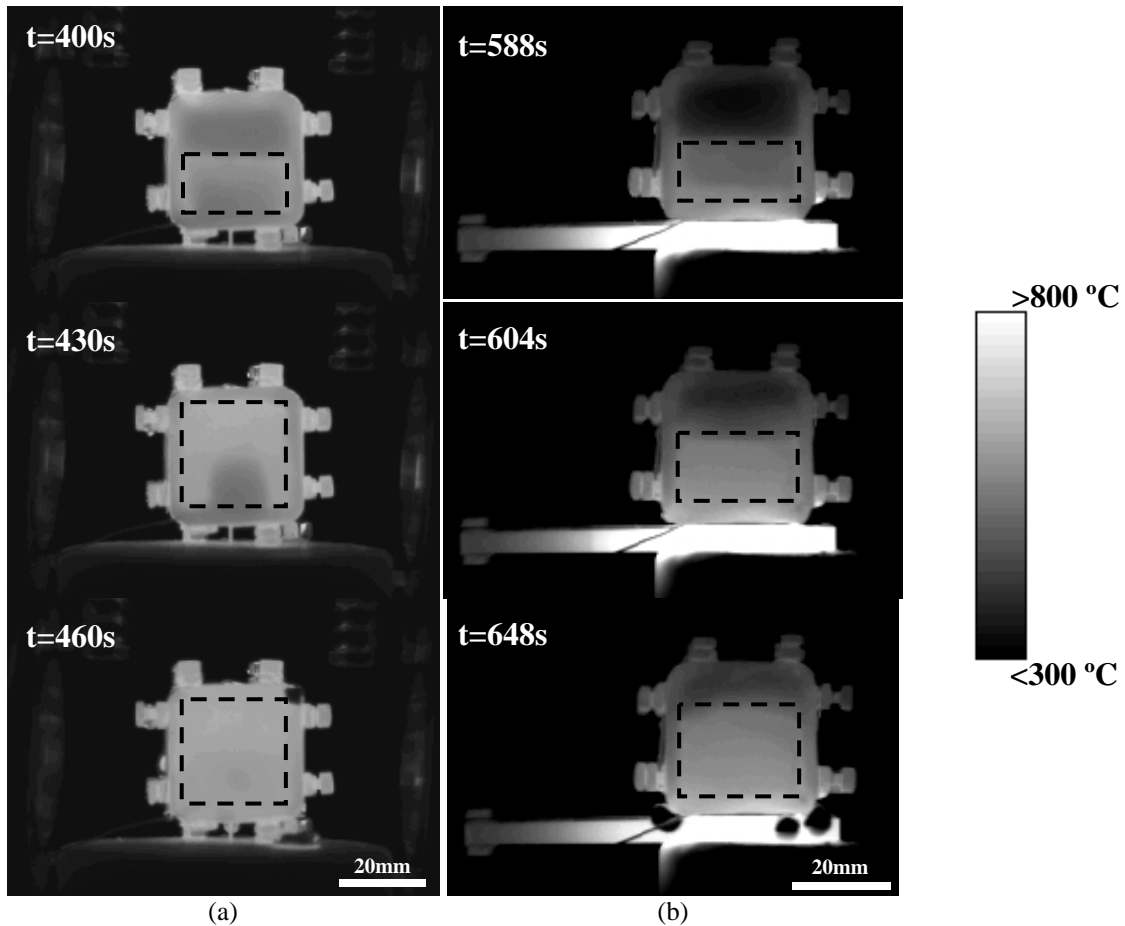


Figure 4

The average temperatures of the foamed zones (indicated in fig.4) for the screened homogeneous heating are  $624 \pm 19$  °C,  $648 \pm 13$  °C and  $664 \pm 9$  °C for the respective increasing foaming times. The average temperatures of the foamed zones for the screened inhomogeneous heating are  $613 \pm 21$  °C,  $659 \pm 14$  °C,  $664 \pm 18$  °C, respectively. In these experiments the standard deviation is related to real temperature gradients more than to temperature inaccuracies and as an example in the second heating condition (b), the

higher standard deviation at  $t=648$  s is related to the higher temperature gradient induced by inhomogeneous heating. These results confirm that mould foaming with a screening foil gives much better, more accurate and reliable temperatures compared to direct monitoring.

### 3.2 Molten state

After the foam has reached its final expansion stage and is kept in the liquid state at  $660$  °C, direct IR monitoring of these foams shows several noticeable features such as hot spots (1), fresh surfaces (2) and reflexions (3) (see Fig. 5). It was not possible to obtain reliable quantitative thermographies from such experiments since the apparent temperature differences between various parts of the surface were unrealistically high, as demonstrated by the high standard deviation of the average temperature of the surface. The temperature of the hot spots (1) was 80% higher than the temperature around them, while the temperature of the fresh foam surfaces (2) was merely half the average value. The reflection (3) of the heating ceramic plate situated in the bottom is another important contribution that distorts the temperature reading in the lower parts of the image.

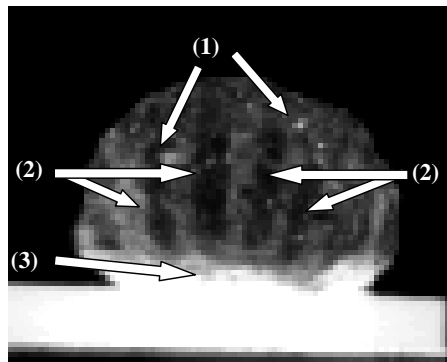


Figure 5

The observed artefacts in the thermographic images are partially an effect of the different surface roughnesses and curvatures. The hot spots can be explained by considering that burst bubbles at the surface focus the energy through the concavity and thus radiate more energy through a small hole than the average energy corresponding to the whole inner surface. In addition to these effects, the influence of varying emissivity due to the different grade of oxidation of the fresh surfaces compared with the initial surface gives rise to varying temperature readings although the real temperature is constant.

The assumed additional effect of progressive oxidation was studied on a reference sample made of pure (99.9 %) aluminium (not a foam) that was melted and kept at a high constant temperature for an extended period (600 s). As a consequence, an apparent temperature increase was registered –shown in fig.6– while the real temperature was kept constant at 660°C. The emissivity was initially adjusted to 0.25 to obtain the same temperature value in both thermographic camera and reference thermocouple. The graph shows the apparent surface temperature increase, reaching after 10 min an apparent temperature of roughly the double. Thus, this is an effect of progressive surface oxidation reflecting an increase of emissivity. Therefore, we can consider that the progressive oxidation of the surface is another important factor to consider in long time experiments for the direct monitoring of the aluminium foaming process even though calibration curves could be used in controlled conditions.

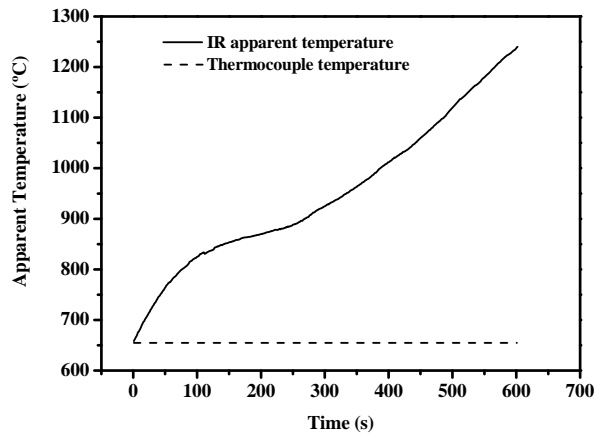


Figure 6

As already demonstrated, the screening method allows for measuring a reliable IR temperature and it is possible to determine the real temperature distribution even when the foam is in the liquid state. The thermal images obtained were analysed and it was found that only in the vertical (Z) direction the temperature variations were significant. This can be explained by the symmetry of the heating configurations applied. The temperature profile does not change significantly with time any more after the foam has expanded to its maximum, i.e. the distribution is stationary, when the foam is kept at an average constant temperature of 660 °C.

The stationary temperature distributions along Z in the marked rectangle are plotted in Fig. 7. In Fig. 7a the time averaged thermal image and the temperature profile obtained when heating the sample with three infrared lamps (“uniform heating”) are shown. The maximum difference in temperature from bottom to top is below 25 °C. Inhomogeneous heating (Fig. 7b) yields higher temperature differences from the bottom to the top. A pronounced temperature drop is found in the top part, probably related to the absence of contact between the foam and the steel foil. As a consequence, the temperature in this

area is much lower than expected, reaching a value below the melting point, and obviously not representing the true temperature of the foam. The expected temperature is also displayed in Fig. 7. The maximum temperature difference from bottom to top is about 90 °C, and the temperature profile is approximately linear under the inhomogeneous stationary heating conditions applied.

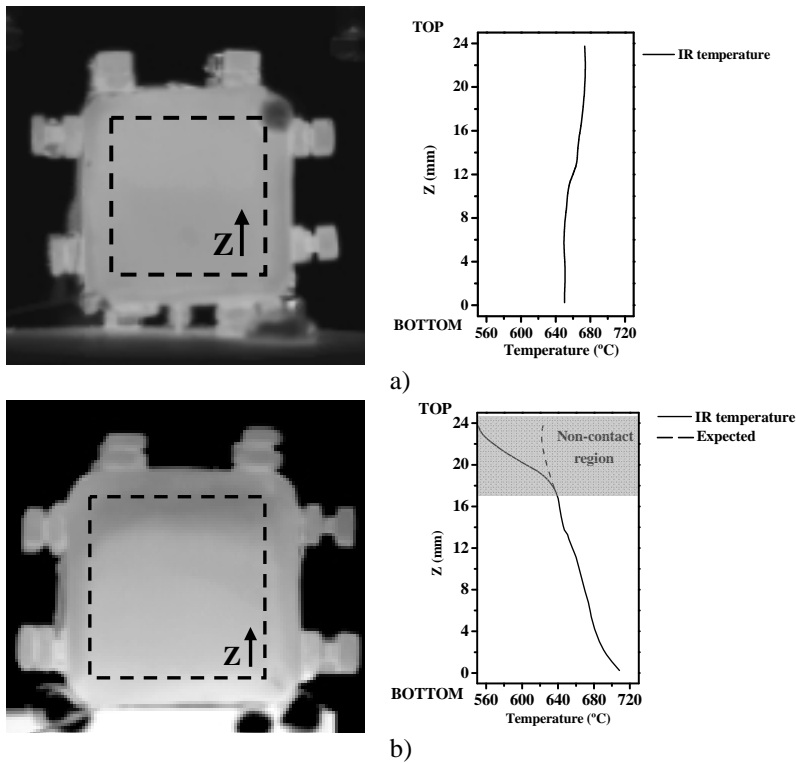


Figure 7

The maximum temperature differences and the temperature profiles are clearly different when these two heating conditions are applied, but it is important to note that both samples were kept at the same average constant temperature of about 660 °C. The temperature differences under homogeneous heating conditions are low but are far from being constant.

### 3.3 Solidification

After having kept the sample in the molten state for 600 s the heaters were disconnected and the samples were allowed to cool down. The transition from liquid to solid can be monitored with thermocouples and appears as a reduction in the cooling rate since the latent heat is released. As a consequence, a change in the slope of the temperature course would be expected during solidification but in practice this change of slope is masked by the high heat capacity of the steel mould even though we ensured that the foam was in direct contact with the sample. In contrast, in the case of free foaming (unscreened sample), it is possible to follow the phase change which appears as a “solidification wave”. In Fig. 8 three stages of solidification of a liquid sample can be clearly discerned. The phase change observed is just opposite to the expected change since solidification seems to enhance the emissivity because the apparent temperature of the solidifying part of the foam appears higher than that of the molten part. In Fig. 8 we can see how the sample starts to solidify in the top part and solidification propagates from top to bottom. As mentioned, the solid foam shows an *apparently* higher temperature (is brighter), whereas the molten part exhibits an apparently lower temperature. These results are in accordance with those found by other researchers during monitoring of the solidification process of other materials with a thermographic camera. This kind of results are possible when the solid phase shows a higher emissivity than the liquid one <sup>[23,24]</sup>. The average solidification speed calculated from this image series is roughly 3.75 mm/s for a sample mass of 4.5g.

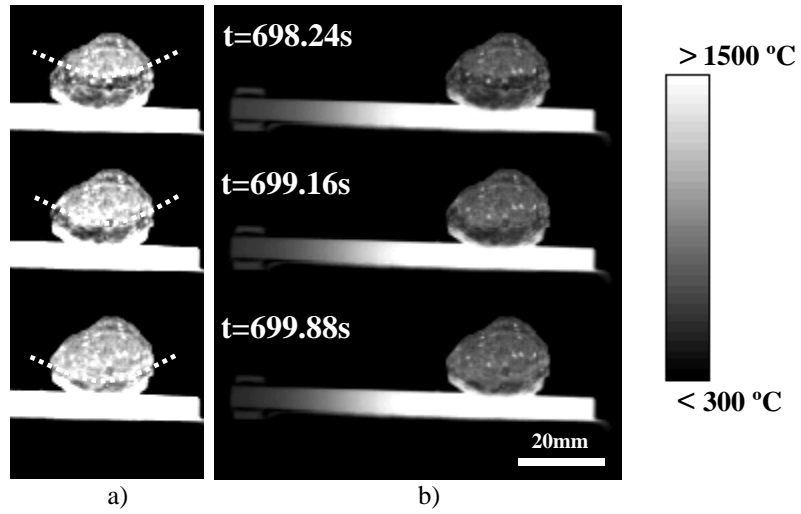


Figure 8

## 4 SUMMARY and OUTLOOK

A thermographic technique has been applied to study the temperature distribution during expansion, in the liquid state and during solidification of aluminium foams. It was found that:

- Measuring the temperature profile of an open metal foam surface directly yields merely a qualitative picture of the thermal conditions. The temperature reading is distorted by geometrical changes of the sample and variations of the surface emissivity caused by different oxidation grades.
- By measuring the temperature of a liquid foam indirectly through a thin screening metal foil in contact with the foam we could obtain a reliable and quantitative data set representing the true spatial and temporal temperature field of the liquid metal foam.
- Inhomogeneous heating conditions gave rise to localized early foaming in some regions and lower final expansions of the unit foam, whereas homogeneous heating conditions yielded homogeneous and fast early foaming and higher final expansions. The molten foam is stable and presented a stationary temperature distribution while kept at 660 °C for 600 s.
- The solidification progress was possible to be monitored thanks to a distinct surface emissivity of solidifying regions. This phenomenon could be only appreciated in direct monitoring conditions. Solidification of the small pieces of foam studied occurred in less than 4 seconds.

In the future, the effect of temperature and its distribution on the liquid metal foam could be further studied by simultaneously combining thermography with other in-situ characterisation methods such as X-ray radioscopy <sup>[25]</sup>. In this way, it would be possible to correlate features of the temperature distribution with internal processes in the foam such as the redistribution of melt (drainage) and cell wall rupture (coalescence).

## **ACKNOWLEDGEMENTS**

The authors are grateful to the Spanish Ministry of Science and Education that supported the stay of E. Solórzano in Berlin with a FPU grant Ref-AP-2004-2908. Additionally, the authors thank Admatis Ltd. Miskolc, Hungary, who generously supplied the IR camera used in this work. Funding by the European Space Agency ESA (Projects  $\mu$ g-FOAM AO-99-075 and XRMON AO-2004-046) is also gratefully acknowledged.

## REFERENCES

---

- [1] J. Banhart, Manufacture, characterization and application of cellular metals and metal foams, *Prog. Mater. Sci.* 46, 2001, 559–632
- [2] K.Y.G. McCullough, N.A. Fleck And M.F. Ashby, Uniaxial stress-strain behavior of aluminium alloy foams, *Acta Mater.* 47, 1999, 2323–2330
- [3] C. Körner, M. Arnold, R. F. Singer, Metal foam stabilization by oxide network particles, *Mat. Sci. Engnr. A* 396, 2005, 28–40
- [4] C. Körner, M. Hirschmann, V. Bräutigam, R.F. Singer, Endogenous particle stabilization during magnesium integral foam production, *Adv. Engnr. Mater.* 6, 2005, 385–390
- [5] N. Babcsán, D. Leitmeier, H.P. Degischser, Foamability of particle reinforced aluminium melt, *Matt.-Wiss- u. Werkstoffech* 34, 2003, 22–29
- [6] J. Banhart, Metal foams: Production and stability, *Adv. Engnr. Mater.* 8, 2006, 781–794
- [7] V. Gergely, B. Clyne The FORMGRIP process: Foaming of reinforced metals by gas release in precursors, *Adv. Engnr. Mater.* 2, 2000, 175–178
- [8] D. Bryant et al., Method for producing foamed aluminum products by use of selected carbonate decomposition products, US patent application 2006/0243094 A1
- [9] C. Körner, M. Hirschmann, H. Wiehler, Integral Foam Moulding of Light Metals, *Mater. Trans.* 47, 2006, 2188–2194
- [10] E. Solórzano, J. A. Reglero, M. A. Rodríguez-Pérez, J. A. de Saja ,M. L. Rodríguez-Méndez Improvement of the foaming process for 4045 and 6061 aluminium foams by using the Taguchi methodology, *J. Mater. Sci.* 42, 2007, 7227–7238
- [11] B. Matijasevic-Lux, J. Banhart, S. Fiechter, O. Görke, N. Wanderka, Modification of titanium hydride for improved aluminium foam manufacture, *Acta Mater.* 54 ,2006, 1887–1900
- [12] F. von Zeppelin, M. Hirscher, H. Stanzick, J. Banhart, Desorption of hydrogen from blowing agents used for foaming metals, *Comp. Sci. Techn.* 63, 2003, 2293–2300
- [13] Th Wübben, H Stanzick, J Banhart S Odenbach, Stability of metallic foams studied under microgravity, *J. Phys.: Condens. Matter* 15, 2003, S427–S433
- [14] H.M. Helwig, J. Banhart, In: Cellular metals and metal foaming technology, Editors: J. Banhart, N.A. Fleck, A. Mortensen, pp. 165-168, MIT-Verlag, Berlin (2003)
- [15] B. Linnander, When it's too hot to touch use infrared thermography, *Circuits and Devices Magazine*, IEEE 9, 1993, 35-37
- [16] M. Speka, S. Mattei, M. Pilloz, M. Ilie, The infrared thermography control of the laser welding of amorphous polymers, *NDT & E International* 41, 2008, 178-183
- [17] G. Brügemann, A. Mahrle, Th. Benziger, Comparison of experimental determined and numerical simulated temperature fields for quality assurance at laser beam welding of steels and aluminium alloying, *s NDT&E International* 33, 2000, 453–463
- [18] H. Haferkamp, F.-W. Bach; M. Niemeyer, R. Viets, J. Weber, M. Breuer, T. Krussel, Tracing thermal process of permanent mould casting; *Proc. IEEE Int. Symp. Industrial Electronics* 3(3), 1999, 1442–1447
- [19] U. Netzelmann, M. Abuhamad and G. Walle, Thermographic observation of heat transport in solid foams, *J. Phys. IV France* 125, 2005, 511–513
- [20] X.P.V. Maldague. *Theory and Practice of Infrared Technology for Nondestructive Testing*, John Wiley & Sons. New York, 2001
- [21] P. M. Reynolds, Spectral emissivity of 99.7% aluminium between 200 and 540° C, *Br. J. Appl. Phys.* 12, 1961, 111–114
- [22] M.D Abramoff, P.J. Magelhaes, S.J. Ram, Image Processing with ImageJ. *Biophotonics Int.* 11, 2004, 36–42.
- [23] Q.-Q. Tang, G.-C. Huang, The research and application of phase change thermography technique, *Exp. Measurements Fluid Mech.* 17, 2003, 15–17.
- [24] K. Nagashio, H. Murata, K. Kuribayashi, In situ observation of solidification behavior of Si melt dropped on Si wafer by IR thermography, *J. Cryst. Growth* 275 ,2005, e1685–e1690

- 
- [25] F. García Moreno, M. Fromme, J. Banhart, Real-time X-ray radiography on metallic foams using a compact micro-focus source *Adv. Engnr. Mater.* 6, 2004, 416–420